Paste 2024 – AB Fourie & D Reid (eds)

doi:10.36487/ACG_repo/2455_21

# Exploring the role of time-dependency in tailings deposition flows

**AM Talmon** *Deltares, and Delft University of Technology, The Netherlands*

**M Nabi** *Deltares, The Netherlands*

**E Meshkati** *R&D Boskalis (formerly with Deltares), The Netherlands*

## Abstract

*In the field of fluid dynamics, initial focus is often placed on steady flow conditions. However, an intriguing phenomenon emerges when we observe that flow behaviour in deposits can be time dependent. While the deposition of coarse particles might seem an obvious contributor to this phenomenon, it's important to note that time-dependent flow also occurs in flocculated or coagulated, fine, non-settling materials. This prompts us to explore the possibility of time-dependency in homogeneous non-Newtonian fluids, considering two key aspects: changes in rheological properties and variations in fluid flow characteristics over time.*

*An initial comparison by Talmon et al. (2023) of two different time-dependent rheology models revealed similar behaviour but also showed intriguing differences in numerical calculation of beach deposition's straight channel flow, which demanded further investigation. We reveal the origin of differences, recalculate and converge results. These two models concerned reversible time-dependency, e.g. thixotropy. Rheomalaxis, e.g. irreversible time-dependency of rheological properties, will be addressed too.*

*With shear thinning of tailings, deposition conditions appear prone to the development of surface waves. The flow conditions in open channel flow experiments and a tailings flume deposition trial are analysed by means of numerical fluid flow simulation (time-independent rheology) and indeed, surface level variations are calculated. This corresponds qualitatively with observed variation of plunge pool level and irregular flow.*

*Tailings are flocculated to speed up dewatering. Our studies show that it is also necessary to quantify associated time-dependent rheological properties because flocculation highly influences deposition flow. Our calculations show that flocculation affects both the depth of streams as well as their velocity. In 3D, relating to earlier devised analytical channel formation theory (Talmon 2023), it may initiate pattern formation and affect run-out distances. Dedicated flocculation might be a way to influence and manage deposition; when we better understand the flow path of the material.*

**Keywords:** *tailings storage facility, rheology, thixotropy, rheomalaxis, computational fluid dynamics, free surface waves, validation*

## 1 Introduction

Mine tailings generally contain high concentrations of coarse and fine particles. Their proportion and material differs per mine and operation. Constituents and behaviour of constituents are different in rock mining compared to, for instance, oil sands mining where the role of fines is dominant. Despite differences, discharged tailings follow and create their own flow paths. It is important to deposition management to understand the origin of this behaviour and to be able to predict it. Two obvious candidates are settling of the coarse fraction, like in shaping riverine systems, and time-dependency of rheological properties. The combination of both is present in many thickened tailings streams. A particular class are the fluid fine tailings (FFT) such as in oil sands. These FFT are (re)flocculated, contain no settling sand, and upon discharge form pattern.

Availability of predictive tailings deposition models will enable a physics-based management of tailings storage facilities (TSF), dedicated towards shortening time to closure and subsequent landscaping. To reach that, physics must be understood better in relation to the flow and pattern formation. This can only be achieved by a phase-wise approach: stepwise expanding on physical processes, and dimension of the modelling approach. There are currently two lines of numerical flow modelling: settling sands in a shear thinning carrier consisting of fines (Delft3Ds) (Sittoni et al. 2016) and time-dependent rheological modelling without settling sand (Parent & Simms 2019; Talmon et al. 2023).

Very fine particles can flocculate or coagulate. A challenge is that flocculation of clays and other fine particles in modern tailings introduces pronounced irreversible time-dependent properties; the flocculated colloid structure of fines does not immediately adapt to local flow conditions, and it may take some time to recover, or recovery may be incomplete, or may not take place at all. In case of clays, it generally suffices to consider particle sizes less than 44 micron as fine, e.g. the rheological active part of the mixture. For other fine constituents, the discriminative particle size may be different.

The fines as common denominator are a likely candidate for pattern formation, but the settling of sand is also important. It builds the deposit, and the analogy to riverine systems is evident and potentially imposes a greater impact on the overall flowing behaviour of the tailings stream. Theoretically, it is also possible that after an initial segregation of coarse particles, sand settling becomes minimal in the stream and can be neglected.

This paper investigates the influence of time-dependency of tailings rheology so it can be applied to FFT directly, but learnings also apply to tailings with settling sand (or other material) and fines governing rheology.

## 1.1 Problem

There is a huge difference between assuming that the flow spreads uniformly in all directions and formation of preferent channels, observed in many deposits. Depending on tailings composition/properties and discharge conditions different flow regimes develop (Charlebois 2012). Deposition flows are known to build up a sandy bed layer, but attributing pattern formation in TSFs to segregation of sand might not be sufficient, as it might be concluded from numerical calculations performed by the Delft3Ds model (Sittoni et al. 2016: Talmon et al. 2018). A likely candidate for pattern formation is time-dependent rheology. In time-dependent rheology, reversible time-dependency is called thixotropy and irreversible time-dependency is called rheomalaxis. The difference is that in the latter, the internal structure is damaged beyond repair, contrary to the self-healing capacity of the former. Most tailings show rheomalaxis as opposed to true thixotropy. The degree of time-dependency can be substantially different between tailings but is inherent to colloid clays. In addition to sand that settles relatively easy, the fines may be subject to settling/dewatering too.

In deposits, the free surface of flows is also observed to vary in time. Self-formed channels may overflow regularly, hydraulic jumps may form (Pirouz et al. 2015). Plunge pool levels vary with time.

To reduce complexity, we will only look at the behaviour of homogenous material over channel length, so we exclude the sand settling and the slow settling/dewatering of fines. The model described in this paper has time-dependent rheology instead.

Research questions of the current study are:

1. Can wavy surface variation be a factor to be taken into account in the formation of flow pattern, particularly the formation of alternating channels in deposits?
2. Is time-dependent rheology important?
3. Is the choice of thixotropy model critical?

## 1.2 Objective

Our objective is to share our gained understanding of harmonic time-dependent surface level variations systematically found with the model, to update on the comparison between two different time-dependent rheological models, and discuss/demonstrate the relevancy of time-dependency.

## 1.3 Approach

Earlier calculations with time-dependent rheology are reviewed and the influence of time-dependent rheology is quantified. Regarding surface wave development, the major features of the theory are summarised and calculations by the presented research model are compared with the theory, referring to flow conditions in experiments with tailings and alike clay slurries.

The model cannot simulate three-dimensional (3D) flow yet, but there is analytical depth-averaged theory on pattern formation developed (Talmon 2023). Two-dimensional results are projected onto this higher-level depth-averaged approach. Consequences for 3D pattern formation in TSFs are hence briefly discussed.

# 2 Theory

## 2.1 Rheology

The shear thinning rheology of tailings is in our model described by the Herschel-Bulkley (HB) model:

$$\tau = \tau_y + K\left(\dot{\gamma}\right)^n \tag{1}$$

where:

$\tau_y$ = yield stress

$K$ = viscosity index

$N$ = flow index

$\dot{\gamma}$ = fluid shear rate.

In case of rheological time-dependency, the yield stress and the viscosity index are a function of time and space, governed by the calculated structure ($\lambda$) of local colloid clay fabric (Talmon et al. 2023; Talmon & Meshkati 2023). Rheological time-dependency is also referred to as 'thixotropy' when there is a reversible decrease in viscosity with time of shear. The range of conditions is indicated in Figure 1, showing two bounding flow curves according to Equation 1, quantifying unremoulded ($\lambda$=1) and remoulded ($\lambda$=0) conditions. In between we see the equilibrium flow curve (EFC) which is the theoretical curve when the decay rate of structure and the recovery rate are equal.

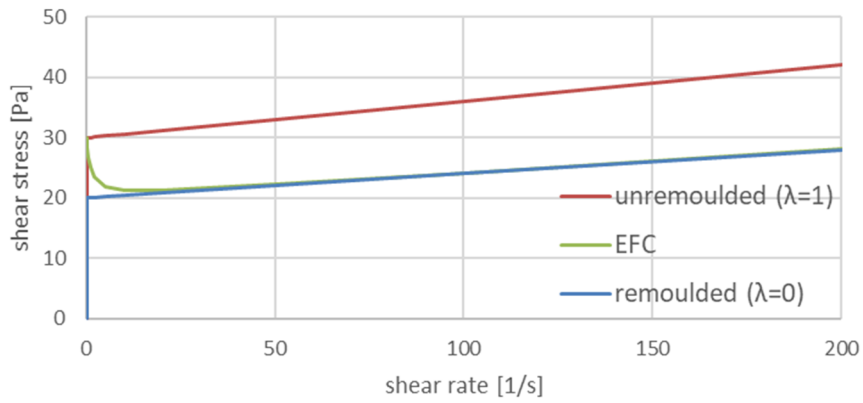


**Figure 1 Rheological concept: rheology at maximum and minimum structure (λ) of colloid clay fabric**

Structure is calculated by means of a kinetic equation by which the change of structure is calculated flowing along with the fluid. In case of the Houska model, it is described by Equation 2, after Moore (1959). Minimum value and maximum value of $\lambda$ are 0 and 1, respectively.

$$\frac{D\lambda}{Dt} = a\left(\lambda_0 - \lambda\right) - b\lambda\left|\dot{\gamma}\right| \tag{2}$$

where:

$\lambda_0$ = maximum structure

$\lambda$ = structure

$a$ = recovery coefficient

$b$ = decay coefficient

$t$ = time.

The kinetic equation utilised in the Parent & Simms (2019) model is:

$$\frac{D\lambda}{Dt} = \lambda / T - \alpha\lambda\left|\dot{\gamma}\right| \tag{3}$$

where:

$T$ = timescale recovery

$\alpha$ = decay coefficient.

In the constitutive equation of Parent & Simms (2019), the yield stress is zero and the flow index n=1. Only the viscosity index K is a function of structure λ.

## 2.2 Kinematic and dynamic waves

Numerical calculations show surface waves. Flow conditions will be evaluated with respect to existing wave initiation theory. The relative dynamic velocity of free surface waves, relative to the mean flow velocity *U,* is:

$$u = \sqrt{gh} \tag{4}$$

where:

$u$ = relative dynamic velocity of waves

$g$ = gravitational acceleration

$h$ = flow depth.

The dynamic velocity quantifies inertia effects but does not involve flow regime nor rheology.

The kinematic velocity of free surface waves follows from the ‘stage equation’ which per unit width reads:

$$q = e\,h^{d} \tag{5}$$

where:

$q$ = flow rate per unit width

$e$ and $d$ = constants.

The theoretical kinematic wave velocity (or flood wave speed) of a HB fluid in laminar flow is, assuming local equilibrium flow (excluding short waves):

$$v = \frac{\partial q}{\partial h} = \frac{(2n+1)(n+1)\tau_w^2}{n\left((n+1)\tau_w + n\,\tau_y\right)(\tau_w - \tau_y)}\frac{q}{h} \tag{6}$$

where:

$v$ = kinematic wave velocity

$\tau_w$ = wall or bottom shear stress.

The Vedernikov number $V$ (Ponce 1991; Chow 1959) is the ratio of relative kinematic and relative dynamic wave speed: $V = (v\text{-}U)/u$. A value of $V$=1 is the criterion for surface wave formation: both types of wave travel at the same speed and amplify each other. At a Vedernikov number of $V$=1, the critical Froude number (F) (Coussot 1994), for developing surface waves is found.

For yield stress fluids flowing slowly, with a significant unsheared plug in the upper part of the flow ($\tau_w/\tau_y$ of order 1), the Froude criterion is low: 0.01 < F < 0.1. For comparison, for laminar Newtonian fluid flow, the criterion is F=0.5 and for a turbulent flow it is higher (F=1.5 to 2).

The Froude number of our numerical flow calculations will be compared to the critical Froude number according to Coussot (= neutral stability criterion) to evaluate the likelihood of surface wave formation. The Froude criterion for wave initiation for $n$=1 (Bingham fluid) and a HB fluid with $n$=0.3 is shown in Figure 2, together with the average conditions in our numerical calculations. The horizontal axis is the dimensionless wall or bottom shear stress and indirectly quantifies the depth of flow compared to the thickness of the unsheared plug in the upper part of the flow through the essential linear shear stress distribution with vertical coordinate.

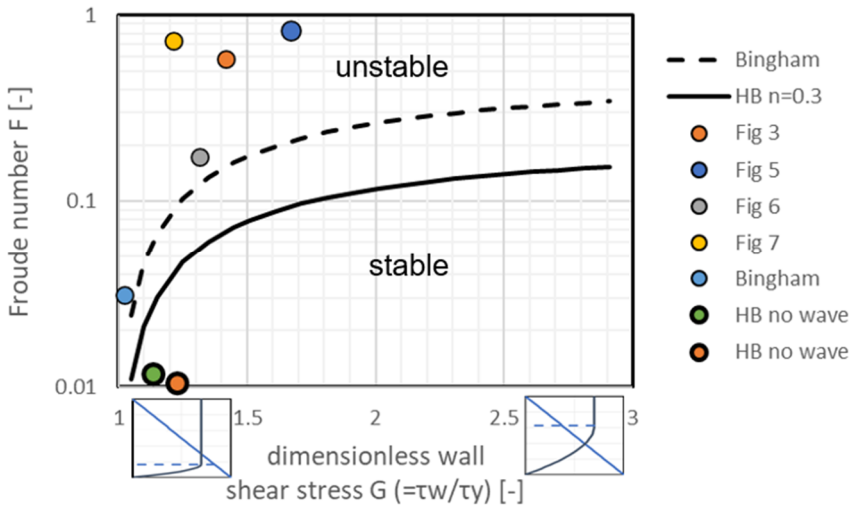


**Figure 2 Free surface wave stability criterion for Bingham model ($n$=1) and Herschel–Bulkley (HB) model (at $n$=0.3), with plotted calculation conditions and indication when no waves were calculated**

Asymptotic behaviour at large $G$-values is not shown in Figure 2, but for vanishing yield stress, theoretical initiation criteria are: F=0.5 (at $n$=1) and F=0.25 (at $n$=0.33). For reference, supercritical (shooting) flow occurs for F>1. For laminar flow, the wave initiation criterion for laminar flow is theoretically in the subcritical regime, F<1. Hence, when hydraulic jumps (F=1) are observed in tailings channels, upstream laminar flow may develop free surface waves already theoretically.

# 3 Numerical flow model

The numerical model presented in this study addresses the intricacies of thixotropic flows, where the rheological behaviour of a mixture of water and clay is modelled. The approach encompasses a comprehensive set of numerical techniques to accurately capture the complex interplay between fluid dynamics and thixotropy.

At the core of the numerical model are the Navier–Stokes equations which describe laminar flow of the water–clay mixture. Augmenting this, a thixotropy transport equation dynamically adjusts the viscosity of the fluid, reflecting changes in its structural state over time. This coupled model enables the simulation of non-Newtonian behaviour characteristic of thixotropic materials.

A Generalised Coordinate System is employed to define the spatial domain, providing a flexible framework to handle intricate geometries encountered in thixotropic flows. The finite volume method is chosen for spatial discretisation, facilitating an accurate representation of spatial variations in the thixotropic mixture. This method ensures robustness in capturing the spatial intricacies inherent in the behaviour of water–soil mixtures.

Temporal evolution is handled using the theta method; a fully implicit time integration scheme. This choice enhances the stability of the simulation which is particularly crucial for representing the time-dependent nature of thixotropic flows accurately. The fully implicit nature of the method allows for a robust handling of the coupled system of equations.

A distinctive feature of the model is its ability to adapt the numerical grid to the deformations of the free water surface. This geometric adaptation is essential for optimising grid resolution in regions where significant changes in the fluid–solid interface occur. By dynamically adjusting the grid, the model ensures that the simulation accurately captures evolving geometries, particularly relevant in scenarios involving free water surface deformations.

To address computational challenges associated with solving the coupled system of equations, a Geometric Multigrid Solver is employed. This solver optimises the convergence of the numerical solution, enhancing the computational efficiency of the model. The Geometric Multigrid Solver is particularly advantageous in dealing with large-scale simulations encountered in the study of thixotropic flows.

Free surface conditions are considered, and appropriate boundary conditions are applied. These conditions are carefully chosen to ensure that the numerical model faithfully represents the physical behaviour of the system under study, accounting for the complexities introduced by the thixotropic nature of the mixture.

# 4 Results

## 4.1 General

Earlier calculations for beach deposition with reversible time-dependent rheology were reviewed. Differences with irreversible time-dependent rheology will be shown. Simulations of actual flume tests were conducted. All of these calculations fall into the surface wave formation regime and for yield shear thinning rheology, the model consistently produces surface waves accordingly. Additional calculations were conducted with smaller bottom slope and other changes to reach non-wave formation conditions. For an overview of utilised model parameter values, see Table 1.

**Table 1 Model parameter values in simulations**

| | Fig 3 | Fig 4 | Fig 5 | Fig 6 | Fig 7 | Only in Fig 2 | Only in Fig 2 | Only in Fig 2 |
|---|---|---|---|---|---|---|---|---|
| Bottom slope: $i$ (-) | 0.02 | 0.02 | 0.02 | 0.0068 | 0.068 | 0.007 | 0.004 | 0.002 |
| Density: $\rho$ (kg/m$^3$) | 1,500 | 1,500 | 1,500 | 1,700 | 1,075 | 1,075 | 1,075 | 1,075 |
| Flow rate: $q$ (m$^2$/s) | 0.1 | 0.1 | 0.1 | 0.01 | 0.002 | 0.002 | 0.0013 | 0.0013 |
| Domain length: $L$ (m) | 200 | 200 | 200 | 25 | 10 | 10 | 10 | 10 |
| Initial depth: $h_0$ (m) | 0.2 | 0.2 | 0.5 | 0.06 | 0.02 | 0.025 | 0.105 | 0.112 |
| $\lambda_i$ structure at inlet (-) | 0.1 | 3 | 0.7 | – | – | – | – | – |
| $\lambda_0$ max structure (-) | 1 | – | 1 | – | – | – | – | – |
| Yield stress at λ=0: $\tau_y$ (Pa) | 30 | – | 20 | 6 | 5.4 | 5.4 | 4 | 2 |
| Viscosity index at λ=0: $\mu$ (Pa s$^n$) | 0.35 | – | 0.3 | 0.1 | 0.004 | 0.004 | 0.35 | 0.35 |
| Yield stress at λ=1: $\tau_y$ (Pa) | 120 | – | 120 | – | – | – | – | – |
| Viscosity index at λ=1: $\mu$ (Pa s$^n$) | 0.85 | – | 20.3 | – | – | – | – | – |
| Flow index: $n$ (-) | 1 | – | 1 | 1 | 1 | 1 | 0.3 | 0.3 |
| Structure self-recovery: $a$ (1/s) | 0.0003 | – | 0 | – | – | – | – | – |
| Structure breakdown: $b$ (-) | 0.0001 | – | 0.0003 | – | – | – | – | – |
| Viscosity regularisation: $m$ (s) | 1,000 | – | 1,000 | 1,000 | 1,000 | 100 | 100 | 100 |
| Viscosity at λ=0: $\mu_0$ (Pa s) | – | 0.36 | – | – | – | – | – | – |
| Non-linearity index: $n$ (-) | – | 1.25 | – | – | – | – | – | – |
| Timescale recovery: $T$ (s) | – | **12** | – | – | – | – | – | – |
| Structure shear down: $\alpha$ | – | **0.001** | – | – | – | – | – | – |

In addition to the information above, more information on models, parameters and symbols is given in Talmon et al. (2023).

## 4.2 Update on thixotropy calculations presented at Paste 2023

The paper at Paste 2023 (Talmon et al. 2023), was the authors' first paper on numerical fluid flow calculations of free surface flow including thixotropy. Responding to an industry question, two rheological models were applied to flocculated oil sands mature fine tailings, implemented in our numerical flow model, and were compared: Parent & Simms's (P&S) (2019) thixotropic rheological model and Houska's (1981) thixotropic rheological model. There were three differences observed:

1. Calculated flow depths (and velocities) were not the same.
2. The surface level varied in both calculations, but varied more and varied differently in Houska's approach.
3. With Houska's model, the flow in the entire domain could suddenly accelerate when a low structure exited the calculation domain, or the flow could nearly come to a halt when high structure exited.

After the Paste 2023 conference, the performance of both rheological models was reviewed and new calculations were conducted. The input of both rheological models is listed in the first two data columns in Table 1. Adapted values are indicated in bold. Earlier calculated flow depths were 0.23 m for Houska and 0.14 m for P&S, now they are both 0.2 m, as visualised by ParaView in Figures 3 and 4.

### *4.2.1. Calculations with Houska thixotropic rheological model*

Upon close inspection of the viscosity subroutine after the Paste 2023 conference, there appeared an implementation problem in the calculation method for structure (λ) in the Houska model. This led to the mentioned greater flow depths and to exaggerated dynamics of the flow.

The new calculation shows a 10% smaller flow depth than in Paste 2023. In these calculations and as shown in Figure 3, we see how low structure at inlet $\lambda$=0.1 (due to pipe flow and plunging for instance) the fluid recovers slowly with distance, except at the bottom, where the material is further sheared down to a lower structure $\lambda$=0.062. Again, there is surface level variation and associated variation of flow velocity, but these are different: less and more harmonically.

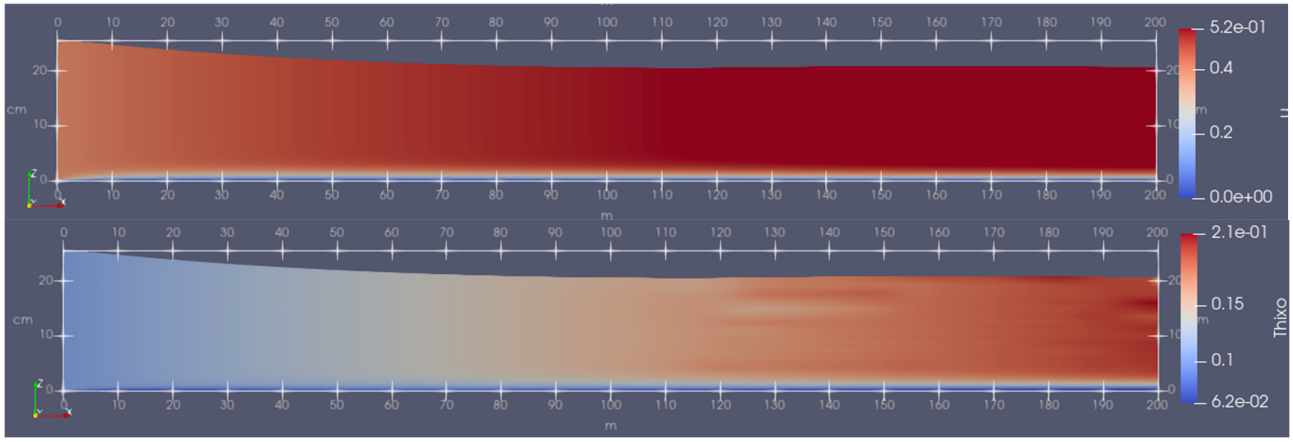


**Figure 3 Flow down a beach. Update for Figure 9 of Talmon et al. (2023) with a new calculation with Houska model**

### *4.2.2 Calculations with Parent & Simms (2019) thixotropic rheological model*

The flow depth calculated with the P&S model at Paste 2023 (Talmon et al. 2023; Figure 3) is lower than in the updated Houska calculation (Figure 3). The difference is traced back to the fitting of P&S rheological parameters. There was no direct fit of the P&S rheological model conducted on the time series of the original rheometry. Instead, the fit was on the calculated EFC (determined by the Houska model that had been fitted earlier to the rheometry (Talmon et al. 2021) and because of the same mathematical formulation of structure decay term, the parameters $b$ and $\alpha$ had been taken the same. The concept that the EFC is the one and only unique representation of the rheology of a thixotropic material was utilised. Although this statement may be true, the timescale is lost in such an approach. When a low structure at the inlet does not recover timely with distance, the result will be a too small flow depth. Hence, keeping the ratio of the growth and decay terms in the kinetic equation the same (so that we are still on the EFC), but shortening the timescale $T$ by a factor of 10, together with increasing the shear down parameter $\alpha$ by a factor 10, the model was run again. Now we calculate the same flow depth as with the Houska model (Figure 4). Notice different colour scale for parameter 'thixo' = $\lambda$, compared to Figure 3.

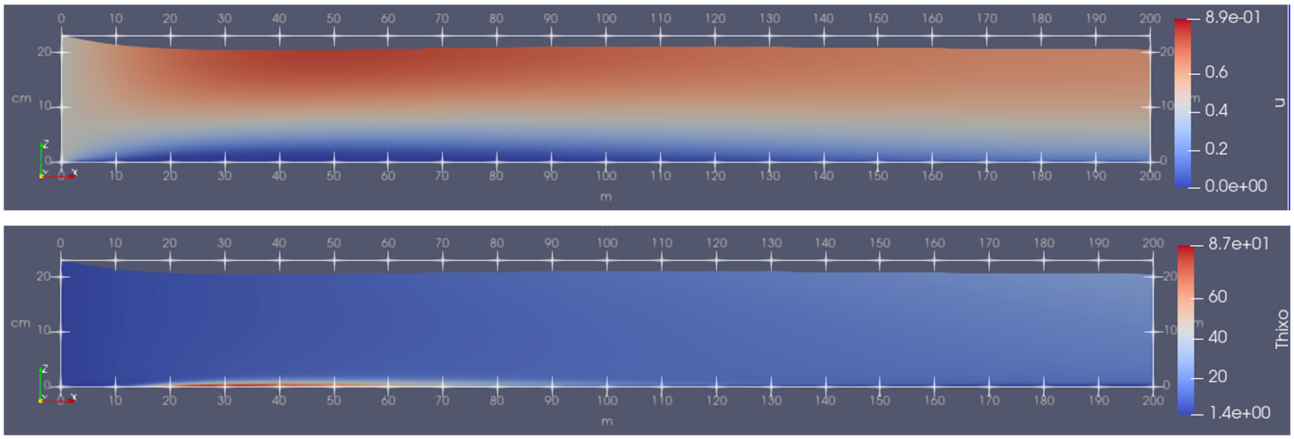


**Figure 4 Update for Figure 10 of Talmon et al. (2023). Parent & Simms model, parameter values in kinetic equation changed by a factor of 10**

## 4.3 Rheomalaxis

With the reviewed numerical model, calculations have also been conducted into the role of irreversible time-dependency (Talmon & Meshkati 2023; Figure 5). The material close to the bottom is irreversibly sheared down. This sheared boundary layer broke up after some distance. The general result is that flow depths are substantially smaller than one would calculate on the basis of flocculated properties. However, calculated flow depths are not as small as for fully remoulded (irreversible) conditions. In the calculation, the self-healing term of the kinetic equation for structure ($\lambda$) was set to zero (so, there was no reversibility possible). A snapshot is shown in Figure 5. Irregular surface variation is experienced, partly synchronous with boundary layer breakup, which was not seen in any other simulation.

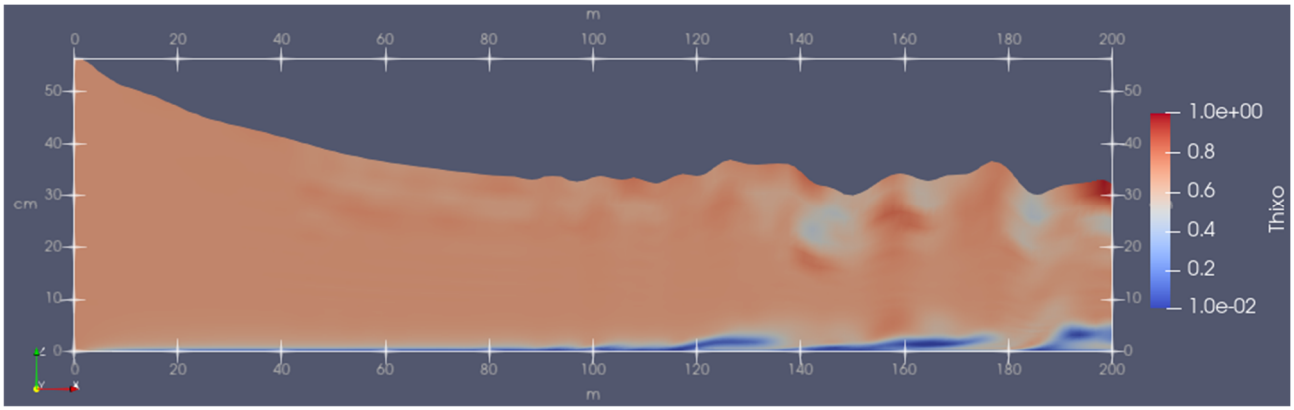


**Figure 5 Rheomalaxis: breakup of boundary layer with irreversible sheared down material at q=0.1 m$^2$/s, captured after 55 minutes. Legend: structure 'thixo=λ'**

## 4.4 Simulation of Sisson et al. (2012) flume test

In Sisson et al. (2012), the flow of prototype tailings in an onsite flume was tested and model results are shown in Figure 6. The flume is 20 m long, 1 m wide with a channel bottom at a constant slope of i=0.0066. The feed consisted of a pipe discharging from higher elevation. A meandering channel developed between tailings banks that stuck to the side walls and plunge pool surface level varied. After rising slowly, this surface level would drop relatively fast when arrested bank material commenced moving again. It seems that strength gain of deposited material is overwon by higher static forcing from the elevated plunge pool level. We are, however, curious if this surface level variation on its own can be understood as a free surface instability. Depth of flow was not measured, the velocity of channeled flow is however back calculated from a series of released floaters, observed channel width and a direct flow velocity measurement. By also using width/depth ratio corresponding with field experiences (Fitton 2007), we estimate flow depth and hence our

flow rate per unit width. The calculated varying surface level is an indication that plunge pool variation can be due to free surface instability. This behaviour is supported by analytical theory. Figure 2 shows conditions plotted marginally above the Bingham criterion for initiation of free surface waves.

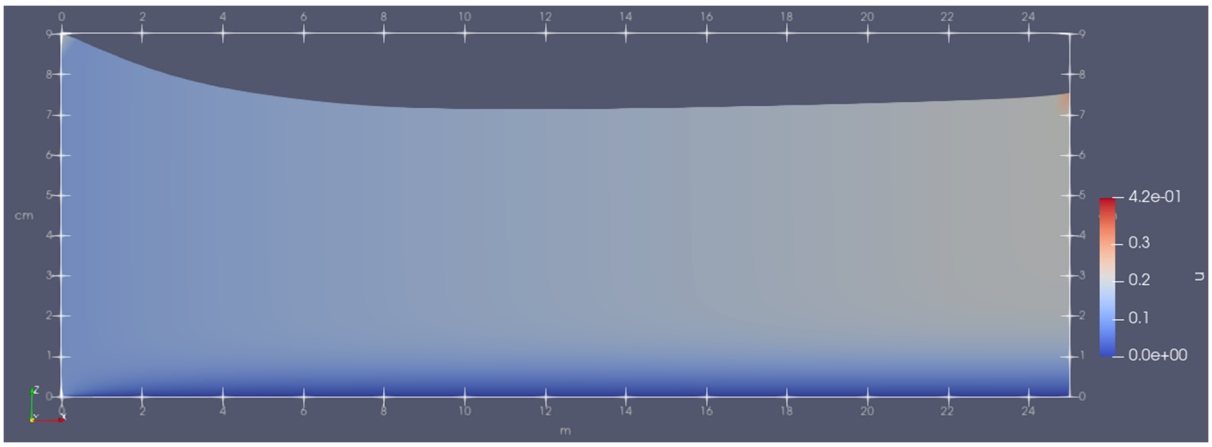


**Figure 6 Calculated velocities for channel flow in Sisson et al. (2012)**

## 4.5 Simulation of some Haldenwang (2003) flume tests

### *4.5.1 Rheology*

Haldenwang (2003) conducted systematic flume tests with two different clay types and carboxymethyl cellulose. In these tests, the rheology was measured by a triplet of pipe viscometers situated in the supply line to the stilling chamber at the flume's inlet. These measured remolded flow curves. There is therefore no information of thixotropy. There was no polymer amended flocculated material involved. Haldenwang's rheometric pipe viscometer data, applying Rabinowitch–Mooney transformation, plots values for true shear rates > 100 (1/s). Haldenwang classified bentonite fluid as a Bingham fluid (on basis of pipe viscometer > 300 (1/s) true shear rate). Fitting on the measured hydraulic resistance of laminar open channel flow itself also allows for a HB fit: $\tau_y$=4 Pa, $K$=0.35 Pa $s^n$, $n$=0.3 and the critical Froude number for such a rheology is lower (Coussot diagram, Figure 2). CMC rheometry was fitted by the power law rheological model and kaolinite rheometry by the HB rheological model.

### *4.5.2 Stability of free surface*

The flume experiments were conducted from laminar transitioning into turbulent flow, but we are only interested in laminar flow. Channel slopes ranged from 1 to 5°. These were full width flume flows, contrary to Sisson et al. (2012). The laminar flow conditions were as well in subcritical flow (F<1), as well as in supercritical flow (F>1).

All bentonite and kaolinite experiments were conducted beyond the criterion for roll wave formation. Our calculations show surface level variations to develop in all three of Haldenwang's testing fluids, bentonite, kaolinite and CMC. For CMC, the authors had to switch to periodic boundary condition between inlet and outlet to have waves develop numerically. An example of calculated laminar flow is shown in Figure 7. Haldenwang on some occasions observed harmonic variation of surface level (Haldenwang, pers. comm., 2023).

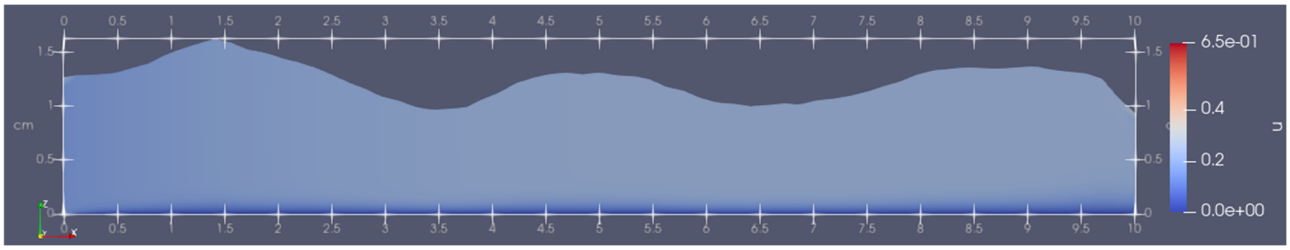


**Figure 7 Example of calculated L=~ 3 m waves at q = 0.002 m²/s , $\tau_y$=5.4 [Pa], μ=0.004 [Pa s], i=0.068 (4° inclined Haldenwang channel)**

The authors ran the numerical model at conditions for further smaller slope and smaller flow rate, and a lower HB yield stress for equilibrium conditions that falls into the stable area of Coussot's graph (Figure 2). The model then ceased to produce waves.

# 5 Evaluation

## 5.1 Calculation domain

The authors' sole focus was on one-dimensional straight channel flow. The flow enters with uniform flow velocity over depth. Calculated surface levels at the inlet are generally a little bit higher than downstream because the flow initially experiences relatively high friction with the bottom. The wall boundary's velocity profile grows with downstream distance, shear rates reduce, and resistance decreases minimally as witnessed by the slight drop of surface level. This may resemble conditions where tailings flow from a plunge pool into a channel.

In comparison to some typical flume tests configurations, the authors have no stilling basin at the inlet of the computational domain which might influence behaviour, nor a discharge in free air at the outlet. In both Sisson and Haldenwang, the flume discharged in free air, hence F=1 at outlet, and associated backwater curves have been measured. In the authors' calculations, only the conditions in the main central part in such a flume were looked at. It is conceivable that the fluid volume available in a stilling basin will dampen oscillations. Outflow might also be dampened if there would be a downstream pond like in TSFs (the model may be extended with such an attribute). In beaching practice, there is a plunge pool upstream and its volume is limited, so our inlet conditions are close to it. In case of the Haldenwang flume, we may for volume regard the first 0.7 m to correspond to storage volume in the stilling chamber. Dynamics, of course, do not correspond here. Hence the model may exaggerate dynamics because some damping might be missing.

## 5.2 Roll wave conditions

The free surface to commences vary in calculations. With time-dependent rheology, the variations become more irregular, and free surface variations and structure changes in the wall bottom layer are interacting. Most of our numerical simulations exceed the theoretical criterion for roll wave initiation.

In all Haldenwang's flume experiments with yield shear thinning fluids (bentonite and kaolinite), the conditions are in the unstable region (Figure 8). Only in some of Haldenwang's CMC measurements are there a couple of conditions in the stable domain of Coussot's graph. CMC is described as a power law, with power between $0.65 < n < 0.95$ ($0.39 < F < 0.49$) and cannot be plotted in Figure 8 because of $\tau_y$ situated in the denominator of $G$.

It is known that roll waves will not necessarily develop in the unstable regime (Coussot 1994). The model had difficulties creating surface wave instabilities with CMC. Oliveira Ferreira et al. (2021) imposed random variations at the inlet to trigger instabilities in the numerical model. Our calculations have not, but we applied the periodic boundary condition. It is conceivable that the strong contrast between the apparent viscosity in the shear layer near the bottom and the high viscosity in plug flow are amplifying instability in simulations with yield shear thinning fluids.

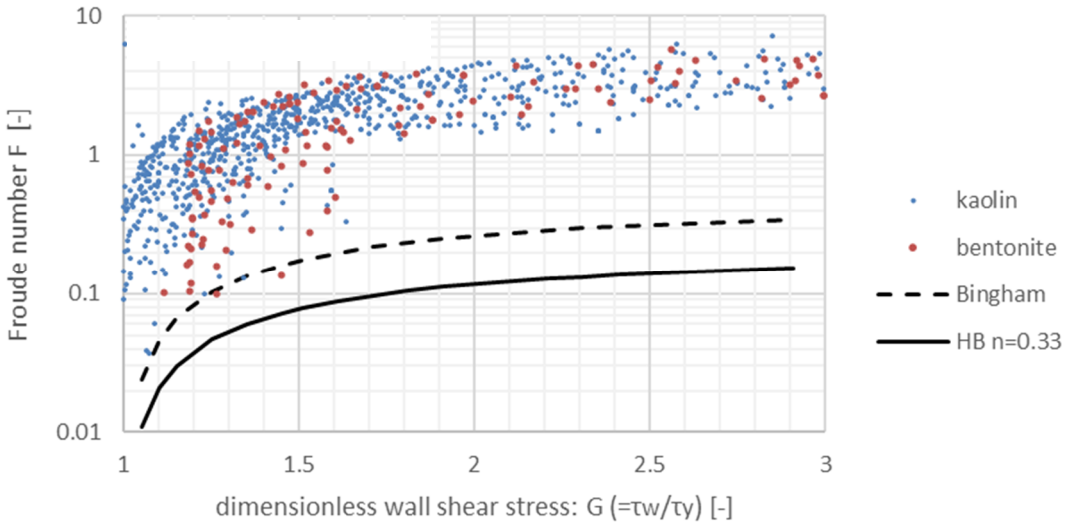


**Figure 8 Flow conditions in Haldenwang flume tests compared to free surface stability criterion**

It cannot be ruled out that the free surface instabilities trigger an early onset of transition to turbulence in straight channels, like Haldenwang measured. Distance of Froude flume conditions to stability criterion could also be a factor (the larger the distance, the stronger the instability). More research is needed.

## 5.3 Analysis time-dependency and analytical theory channel formation

Both Delft3Ds and the applied model produce surface waves. For physics-based settings (beach slope, flow rate, tailings consistency, rheology and sand's shear settling fundamentals), the Delft3Ds model calculates, in 3D already faint pattern in sand concentration in the bottom cells, but channels are not developing yet. So, it might not be the waves (which in theory are full width waves) that trigger basic channel formation. Surface waves within channels might explain overflowing events and plunge pool level variations that might initiate the genesis of new channels.

Linear stability analysis into basic channel formation mechanism of coupled flow and bed formation by shear settling (Talmon 2023) shows that in case of a negative local relation between the bottom shear stress and flow velocity, straight channel formation will prevail. With fluid flow's time-dependency terms neglected, free surface waves are excluded. In this linear stability analysis, the hydrodynamic friction law of variation of bottom shear stress ($\tau_w$) with flow velocity ($u$) and flow depth ($h$) is modelled by:

$$\frac{\tau'}{\overline{\tau}_w} = n\frac{u'}{\overline{u}} - p\frac{h'}{\overline{h}}$$ with linearised friction law: $$n = \frac{u}{\tau}\frac{\partial \tau}{\partial u}$$ and $$p = -\frac{h}{\tau}\frac{\partial \tau}{\partial h}$$

where the prime ' denotes variation with respect to the mean value: overbar ¯ .

For laminar flow of power law fluids it holds $n = p$ which is equal to the flow index of the rheological model, hence the same symbol as in Equation 1 which acquires the same value when the yield stress vanishes.

Referring to the simulation with rheomalaxis (Figure 5) $\Delta h/h$=-15/45 =$\Delta\tau_w/\tau_w$, hence $\Delta u/u$=~1/3. For the analytical theory, this is equivalent to $n$=-1 developing over a distance of about 80 m, and $p$=0 because at this scale there is no causal constitutive frictional relationship between flow depth and bed shear stress. These values need to be super-positioned to the existing small values from fluid flow only (a Bingham flow curve can be approximated by a power law model with power of the order of 0.1). So, for shear thinning fluid this results in $n$=-0.9 and $p$=0.1 corresponding to straight channel formation.

With little or no structure recovery, rheomalaxis is expected to influence pattern formation the strongest. In that case, dedicated flocculation might be a way to influence and manage deposition, but we need to better understand the flow path of the material, and numerical model studies are a way to achieve that.

# 6 Conclusion

After reviewing the implementation of the Houska model and the rheological fit of the Parent & Simms model, beach flow calculations utilising different thixotropy models converge. Despite that, the EFC may be unique to a fluid, and the timescale of structural recovery within the fluid needs to be considered too if the material is expected to recover from upstream conditions, and that may make the difference.

The applied flow model facilitates studies into the role of time-dependent rheology – thixotropy and rheomalaxis – which is important to enable calculation of deposition of treated tailings nowadays. It also reveals time-dependent behaviour of tailings surface level, which is determined by flow conditions in combination with non-Newtonian rheology. Time-dependency is a likely contributor to pattern formation in TSFs and may strengthen the formation of sand deposition pattern that is already calculated for in shear settling alone. Time-dependency may therefore govern cyclic formation of deposition streams and their run-out distance., It is expected that this modelling approach will, if extended to 3D, enable studies into the role of time-dependency with respect to cyclic deposition in tailings storage management. With a strong role of rheomalaxis, dedicated flocculation might be a way to influence and manage deposition when we better understand the flow path of material.

# Acknowledgement

IOSI and COSIA tailings research motivated this further study into time-dependency of deposition flows. Professor Cees van Rhee of Dredging Engineering stimulated research into the flow of clay-sand-water mixtures and subsequent participation in international venues. Walther van Kesteren introduced the first author to tailings storage problems and projects back in 1999. Both Cees and Walther passed away in 2023. The first author is much indebted to them.

# References

Charlebois, LE 2012, *On the Flow and Beaching Behaviour of Sub-Aerially Deposited, Polymer-Flocculated Oil Sand Tailings: a Conceptual and Energy-Based Model*, BSc thesis, University of British Columbia, Vancouver.

Chow, VT 1959, *Open-Channel Hydraulics,* McGraw-Hill, New York.

Coussot, TP 1994, 'Steady, laminar, flow of concentrated mud suspensions in open channel', *Journal of Hydraulic Research*, vol. 32, no. 4, pp. 535–559.

Fitton, T 2007, *Tailings Beach Slope Prediction*, PhD thesis, RMIT University, Melbourne.

Haldenwang, R 2003, *Flow of Non-Newtonian Fluids in Open Channels*, PhD thesis, Cape Technicon, Cape Town.

Houska, M 1981, *Engineering Aspects of the Rheology of Thixotropic Liquids*, PhD thesis, Czech Technical University, Prague.

Moore, F 1959, 'The rheology of ceramic slips and bodies', *Transactions British Ceramic Society*, vol. 58, pp. 470–494.

Oliveira Ferreira, F de, Freitas Maciel, G de & Batista Pereira, J 2021, 'Roll waves and their generation criteria', *Brazilian Journal of Water Resources*, vol. 26, no. 10, p. 202.

Parent, E & Simms, P 2019, '3D simulations of dam breach and deposition using viscosity bifurcation rheology', in J Goodwill, D van Zyl & M Davies (eds), *Proceedings of Tailings and Mine Waste 2019*, Vancouver.

Pirouz, B, Javadi, S, Williams, P, Pavissich, C & Caro, G 2015, 'Chuquicamata full-scale field deposition trial', in R Jewell & AB Fourie (eds), *Paste 2015: Proceedings of the 18th International Seminar on Paste and Thickened Tailings*, Australian Centre for Geomechanics, Perth, pp. 477–489, https://doi.org/10.36487/ACG_rep/1504_37_Pirouz

Ponce, VM 1991, 'New perspective on the Vedernikov number', *Water Resources Research*, vol. 27, no. 7, pp. 1777–1779.

Sisson, R, Lacoste-Bouchet, P, Vera, M, Costello, M, Hedblom, E, Sheets, B,…Sittoni, L 2012, 'An analytical model for tailings deposition developed from pilot-scale testing', in DC. Sego, GW Wilson & NA Beier (eds), *Proceedings of the 3rd International Oil Sands Tailings Conference*, Edmonton, pp. 53–63.

Sittoni, L, Talmon, AM, Hanssen, JLJ, Es, H van, Kester, J van, Uittenbogaard, R, Winterwerp, JC & Rhee, C van 2016, 'Optimizing tailings deposition to maximize fines capture: latest advance in predictive modeling tools', in DC Sego, GW Wilson & NA Beier (eds), *Proceedings of the 5th Int. Oil Sand Tailings Conference, IOSTC*, Lake Louise.

Talmon, AM, 2023, 'Bed pattern initiation in non-Newtonian laminar deposition flow', in RS Sanders & J Schaan (eds), *Proceedings of Hydrotransport 2023,* Edmonton (in press).

Talmon, AM & Meshkati, E 2023, 'Houska based time-dependent rheology model for flocculated tailings', in J Sobota & B Malczewska (eds), *Proceedings of the 20th International Conference on Transport and Sedimentation of Solid Particles,* Wroclaw, pp. 193–205.

Talmon, AM, Meshkati, E, Nabi, M, Simms, P & Nik, RM 2023, 'Comparing various thixotropic models and their performance in predicting flow behavior of treated tailings', in GW Wilson, NA Beier, DC Sego, AB Fourie & D Reid (eds), *Paste 2023: Proceedings of the 25th International Conference on Paste, Thickened and Filtered Tailings*, University of Alberta, Edmonton, and Australian Centre for Geomechanics, Perth, pp. 588–600, https://doi.org/10.36487/ACG_repo/2355_44

Talmon, AM, Meshkati, E, van Kessel, T, Lelieveld, T, Goda, APK & Trifkovic, M 2021, 'On thixotropy of flocculated mature fine tailings: rheometry and lumped structure parameter modelling', in NA Beier, GW Wilson & DC Sego (eds), *Proceedings of Tailings and Mine Waste Conference,* Banff.

Talmon, AM, Hanssen, JLJ, Maren, DS van, Simms, PH, Sittoni, L, Kester, J van, …. Rhee, C van 2018, 'Numerical modelling of tailings flow, sand segregation and sand co-deposition: latest developments and applications', in NA Beier, Wilson GW & DC Sego (eds), *Proceedings of the* 6th *International Oil Sand Tailings Conference,* IOSTC, Edmonton.